

Energy loss in a strongly coupled anisotropic plasma

Kazem Bitaghsir Fadafan^{a1}, Hesam Soltanpanahi^{b2}

^a*Physics Department, Shahrood University of Thechnology, Shahrood, Iran*

^b*National Institute for Theoretical Physics, Gauteng
School of Physics and Center for Theoretical Physics,
University of the Witwatersrand,
WITS 2050, Johannesburg, South Africa*

Abstract

We study the energy lost by a rotating infinitely massive quark plowing, at constant velocity, through an anisotropic strongly coupled $\mathcal{N} = 4$ plasma from holography. It is shown that like the isotropic case the energy deposited either by the drag force or synchrotron radiation of quark in circular motion. We find that the anisotropic parameter has a main effect on the energy lost of heavy quark. We argue that the radiative energy is less than the isotropic case which is interestingly similar to the analogous calculations for the energy loss in weakly coupled anisotropic plasma.

¹e-mail:bitaghsir@shahroodut.ac.ir

²e-mail:hesam.soltanpanahisarabi@wits.ac.za

Contents

1	Introduction	1
2	The gravity background	3
3	Rotating string in a general background	4
4	Rotating string in strongly coupled anisotropic plasma	7
4.1	The energy lost	8
5	Analytic limits	11
5.1	Ultra-relativistic limit	11
5.2	Small a/T limit	14
6	Comparison with linear drag and synchrotron radiation	14
7	Summary and discussion	16
A	Linear drag in a general background	17

1 Introduction

The experiments at Relativistic Heavy Ion Collisions (RHIC) and at the Large Hadron Collider (LHC) have produced a strongly-coupled quark–gluon plasma (QGP)(see review [1]). At a qualitative level, the data indicate that the QGP produced at the LHC is comparably strongly-coupled [2]. The QGP created at the LHC is expected to be better approximated as conformal than is the case at RHIC [1]. The plasma created right after a heavy ion collision is anisotropic for a period of time, $\tau < \tau_{\text{iso}}$ and becomes locally isotropic afterwards [3, 4, 5]. There are no known quantitative methods to study strong coupling phenomena in QCD which are not visible in perturbation theory (except by lattice simulations). A new method for studying different aspects of QGP is the *AdS/CFT* correspondence [1, 6, 7, 8, 9].

The energy loss of partons is a useful probe of the QGP. One should notice that this quantity is not a direct experimental observable, it is manifested in jet quenching parameter \hat{q} . This parameter is a signature of the QGP and initially has been calculated from AdS/CFT correspondence in [10]. Although the energy loss can be due to various different mechanisms, two primary sources of the energy loss are collisions and radiative. The former is due to the scattering of the energetic partons with thermal quarks and gluons in the QGP while the later is related to the Bremsstrahlung radiation during the interactions with the medium. Theoretical study of these phenomena needs strong-coupling tools and non-perturbative methods such as lattice QCD which are inadequate to describe this time-dependent phenomena. A new method is to use the holographic principle and investigate the energy loss of heavy probes.

This method has yielded many important insights into the dynamics of strongly-coupled gauge theories. It has been used to investigate hydrodynamical transport quantities in various interesting strongly-coupled gauge theories where perturbation theory is not applicable. The collisional mechanism of the energy loss of heavy quarks has been initially discussed

using this method in [11, 12]. They considered a heavy quark traveling with constant velocity in linear motion throughout the plasma, and find the energy required to keep it in uniform motion. This energy is then given by the world-sheet momentum that falls across the horizon which is proportional to the momentum of the heavy quark and one concludes that the energy loss mechanism can be considered as drag force. Some extension of this calculation to more realistic models of QGP have been done in [13]. It should be noticed that the physically relevant setting is when there is no external force acting on the energetic parton. Then the moving parton is decelerating, now one finds the possibility of other mechanisms of energy loss which is radiation [14, 15, 16]. Therefore, it would be possible to find interference between two different mechanisms of the energy loss which are the drag force and radiation.

By considering the quark in uniform rotation with constant velocity $v = l\omega$, one can combine two mechanisms of the energy loss. The significant advantage offered by the analysis of this problem was explored in [17]. They determined the energy it takes to move a test quark along a circle of radius l with angular frequency ω through the strongly coupled plasma of $\mathcal{N} = 4$ supersymmetric Yang-Mills (SYM) theory. The drag force and radiation are dominance when $(\omega \rightarrow 0, l \rightarrow \infty, \text{fixed } v)$ and $(\omega \rightarrow \infty, l \rightarrow 0, \text{fixed } v)$, respectively. The extension of this calculation to the case of non-conformal plasma which exhibits a confinement/deconfinement transition at a critical temperature was done in [18]. They argued that in the low temperature, energy loss is completely due to glueball Bremsstrahlung. The motion of a heavy charged quark in a magnetic field was also analyzed in the vacuum of strongly coupled conformal field theory in [19].

In this paper, we study energy lost of rotating quark in a strongly coupled anisotropic plasma. Anisotropic QGP is very important during the initial phase after the production in the heavy-ion collisions. It is related to this point that initially the system expands mainly along the collision axis. As a result the plasma has significantly unequal pressures in the longitudinal and transverse directions. To model this medium, we consider an anisotropic $\mathcal{N} = 4$ SYM plasma in which the x, y directions are rotationally symmetric, but the z direction correspond to the beam direction [20]. The drag force and Jet quenching parameter in this medium were calculated in [23, 24, 25]. It was found that the energy loss of partons depend on the relative orientation between the anisotropic direction and the direction along which the momentum broadening is measured.

Another interesting feature of this anisotropic background is it does not satisfy the known condition for the ratio of the shear viscosity to the entropy density, which is $\eta/s \geq 1/4\pi$.³ While the ratio in transverse direction saturates the KSS bound, it was shown that the perturbation of the metric with an off-diagonal component such (mixing the anisotropy direction with one of the isotropic direction) leads to a smaller ratio, $\eta/s < 1/4\pi$ and, it is a decreasing function of a/T [26].⁴ This is the first example of violation of KSS bound not involving higher derivative theories of gravity [28]. Also they showed that the DC conductivity along (transverse) to the anisotropy direction is a decreasing (increasing) function of the ratio of the anisotropy parameter to the temperature.

Motivated by these considerations, in this paper we study the effect of anisotropy on the energy loss of heavy quark propagating through anisotropic medium. We consider the quark in uniform rotation with constant velocity $v = l\omega$ in the xy plane and discuss two

³ $1/4\pi$ is the KSS bound [27] for this ratio.

⁴As in [20] we identify the temperature and the anisotropy parameter of the plasma by " T " and " a ", respectively.

possible mechanisms of the energy loss. We will compare our results with the results for the drag force and Jet quenching parameter in the presence of anisotropy in the last section.

The article is organized as follows. In the next section, we introduce the anisotropic gravity dual. Then we will give a general discussion on rotating string in a general geometry in section 3. This section will be very useful from technical point of view for our calculations. In section 4, we solve equation of motion of rotating string in the anisotropic background numerically and find the energy lost of heavy quark. Analytic limits will be studied in section 5 and comparison with linear drag and radiation will be done in section 6. Finally, in the last section we discuss our results together with possible extensions for future work. In appendix A we give a fast general review on drag force which is very useful for comparing our results in special limit.

2 The gravity background

We use the anisotropic background which has been introduced in [20]. By a θ term, they deform $\mathcal{N} = 4$ SYM. This deformation parameter in the field theory depends on the anisotropic direction as $\theta = 2\pi n_{D7} z$, where z is the anisotropic gauge theory coordinate and n_{D7} can be thought as the density of D7-branes homogeneously distributed along the anisotropic direction. The D7-brane smear the S^5 part and two spacial directions on the AdS_5 part (xy -plane).

The type IIB supergravity solution in the string frame is given by⁵

$$ds^2 = \frac{L^2}{u^2} \left(-\mathcal{F}\mathcal{B}dt^2 + dx^2 + dy^2 + \mathcal{H}dz^2 + \frac{du^2}{\mathcal{F}} \right) + ds_{S^5}^2$$

$$\phi = \phi(u), \quad \chi = a z, \quad (2.1)$$

where the dilaton field and the axion field are ϕ and χ , respectively, and the anisotropic parameter $a = \frac{g_{YM}^2 n_{D7}}{4\pi}$. The metric functions are also \mathcal{F}, \mathcal{B} and \mathcal{H} which depend on the holographic radial coordinate u and anisotropic parameter a . \mathcal{F} is the blackening function, $\mathcal{F}(u_h) = 0$, and the solution is asymptotically AdS_5 when $\mathcal{F}_b = \mathcal{B}_b = \mathcal{H}_b = 1$. We choose the range $0 < u < u_h$ for the holographic radial coordinate so the boundary theory lives on $u = 0$. The solutions of equations of motion are specified by two parameters, the horizon radius, u_h and the value of dilaton at the horizon, ϕ_h . From boundary theory point of view these parameters map to the temperature, T , and the anisotropy parameter, a . One finds in Fig. 1, two solutions for different combinations of the parameters: Left $\phi_h \simeq -0.22$ and $u_h = 1$ (or $T \simeq 0.33$ and $a/T \simeq 4.4$), Right $\phi_h \simeq -1.86$ and $u_h = 1$ (or $T \simeq 0.48$ and $a/T \simeq 86$).

The metric functions are parameterized by two parameters, the dilaton field value at the horizon ϕ_h and u_h or equivalently by T and a/T . At small a/T , the entropy density scales as in the isotropic case $S_i = \frac{\pi^2}{2} N_c^2 T^3$. At large a/T it scales as $S_a = c_{ent} N_c^2 a^{1/3} T^{8/3}$ where c_{ent} is a constant. To compare our results in the anisotropic plasma to that in the isotropic plasma, one may consider two different ways: the two plasmas can be taken to have the same temperatures but different entropy densities, or the same entropy densities but different temperatures.

⁵This is the finite-temperature generalization of the type IIB supergravity solution of [21], the drag force calculation in this case has been studied in [22].

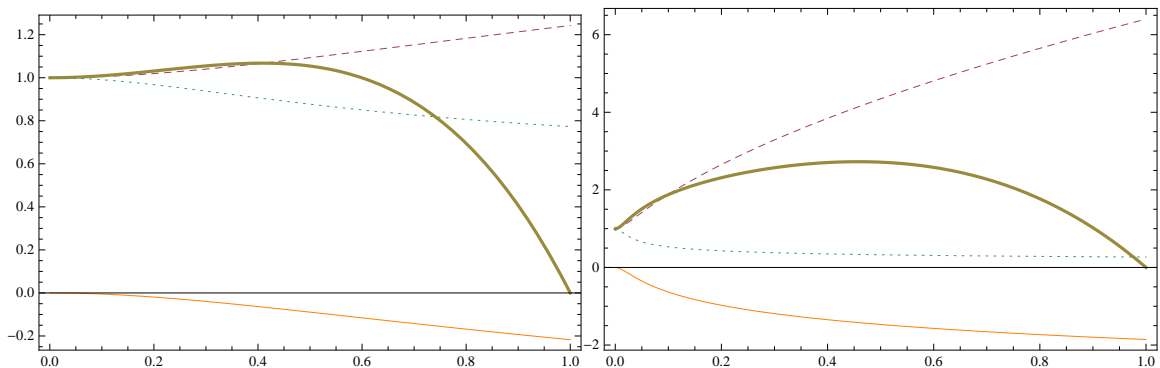


Figure 1: Metric functions ϕ (orange), \mathcal{H} (dashed), \mathcal{F} (thick), \mathcal{B} (dotted) for two different parameters. Left: $a/T \simeq 4.4$, Right: $a/T \simeq 86$.

The field theory coordinates at the boundary are (t, x, y, z) and there is a rotational symmetry in the xy plane. We will consider our rotating test quark in this plane which can be interpreted as transverse plane. One finds that although quark is moving in this plane, anisotropic parameter has main effect on the transport properties of it.

3 Rotating string in a general background

In this section, we will give technical points for studying rotating string in a general background. We will use the results of this section during our calculation in the next sections.

We assume a general form of the static metric as

$$ds^2 = G_{tt}dt^2 + G_{\rho\rho}d\rho^2 + G_{\psi\psi}d\psi^2 + G_{zz}dz^2 + G_{uu}du^2, \quad (3.1)$$

In our coordinates, u denotes the holographic radial coordinate of the black hole geometry and t, ρ, ψ and z label the directions along the boundary at the boundary $u = 0$.

In the gravity dual, a heavy test quark corresponds to an open string with one endpoint on a D3-brane at $u = 0$. The string hangs down into the bulk, extending towards the black-hole horizon at $u = u_h$. In order to study the energy lost for a quark moving in a circle, we must first find the world-sheet of the string spiraling downward from the quark moving on a circle at $u = 0$ and then calculate the energy flowing down the string. We choose to parameterize the two-dimensional world-sheet of the rotating string according to

$$X^\mu(\tau, \sigma) = (t = \tau, u = \sigma, \psi = \omega t + \theta(\sigma), \rho = \rho(\sigma), z = 0), \quad (3.2)$$

where μ runs over five dimensions of the boundary field theory. The Nambu-Goto action is

$$S = -\frac{1}{2\pi\alpha'} \int d\tau d\sigma \mathcal{L} = -\frac{1}{2\pi\alpha'} \int d\tau d\sigma \sqrt{-\det g_{\mu\nu}}, \quad (3.3)$$

where the world-sheet metric is the induced metric from background, $g_{\mu\nu} = G_{MN}\partial_\mu X^M\partial_\nu X^N$. Using the general form of the metric (3.1) and the rotating string's ansatz (3.2), one can show that the Nambu-Goto Lagrangian is given by

$$\mathcal{L} = \left[-G_{uu}(G_{tt} + G_{\psi\psi}\omega^2) - G_{\rho\rho}(G_{tt} + G_{\psi\psi}\omega^2)\rho'^2 - G_{tt}G_{\psi\psi}\theta'^2 \right]^{1/2} \quad (3.4)$$

Here, the prime denotes a derivative with respect to the bulk variable u .

Since the θ dose not appear explicitly in the action, the momentum conjugate to this field is constant and the equation of motion for θ is given by

$$\Pi = \frac{\partial \mathcal{L}}{\partial \theta'} = -\frac{G_{tt}G_{\psi\psi}\theta'}{\mathcal{L}} = \text{const.} \quad (3.5)$$

or equivalently

$$\theta'^2 = -\Pi^2 \frac{(G_{tt} + G_{\psi\psi}\omega^2)(G_{uu} + G_{\rho\rho}\rho'^2)}{G_{tt}G_{\psi\psi}(G_{tt}G_{\psi\psi} + \Pi^2)}. \quad (3.6)$$

where Π is the momentum conjugate to the angular coordinate ψ . The LHS of above equation is positive definite so, the RHS should behave in similar manner. Because we consider the string to stretch from boundary to horizon, so the RHS has a critical point which is the point that both numerator and denominator change the sign and the overall sign of the RHS doesn't change. This critical point is called as u_c and defined by

$$G_{tt}(u_c) + G_{\psi\psi}(u_c)\omega^2 = 0, \quad (3.7)$$

$$G_{tt}(u_c)G_{\psi\psi}(u_c) + \Pi^2 = 0. \quad (3.8)$$

which leads to

$$|G_{tt}(u_c)| = \Pi\omega, \quad |G_{\psi\psi}(u_c)| = \frac{\Pi}{\omega}. \quad (3.9)$$

For the usual case of isotropic background which was studied in [17], the geometry is given by

$$ds^2 = \frac{1}{u^2} \left(-(1 - \pi^4 T^4 u^4) dt^2 + d\rho^2 + \rho^2 d\psi^2 + dz^2 + \frac{u^4 du^2}{(1 - \pi^4 T^4 u^4)} \right), \quad (3.10)$$

and one finds from (3.7) and (3.8) that

$$u_c = \frac{1}{\pi^2 T^2} \sqrt{-\frac{\Pi\omega}{2} + \frac{1}{2} \sqrt{\Pi^2\omega^2 + 4\pi^4 T^4}}, \quad (3.11)$$

$$\rho_c = u_c \sqrt{\frac{\Pi}{\omega}}, \quad (3.12)$$

This is the same as the critical values in [17].⁶

Now we assume that the general background in (3.1) has the SO(2) symmetry on xy -plane and reduces to

$$ds^2 = f(u) (g(u)dt^2 + d\rho^2 + \rho(u)^2 d\psi^2 + h(u)du^2) + G_{zz}(u)dz^2. \quad (3.13)$$

We then obtain the equation of motion for $\rho(u)$ as follows

$$\begin{aligned} & 2g^2 h^2 (\Pi^2 - \omega^2 f^2 \rho^4) \\ & - [h\rho^3 (-2fg^2 (g + \omega^2 \rho^2) f' + (\Pi^2 \omega^2 - f^2 g^2) g') + g\rho (g + \omega^2 \rho^2) (\Pi^2 + f^2 g \rho^2) h'] \rho' \\ & + 2g^2 h (\Pi^2 - \omega^2 f^2 \rho^4) \rho'^2 \\ & + \rho^3 [2fg^2 (g + \omega^2 \rho^2) f' + (-\Pi^2 \omega^2 + f^2 g^2) g'] \rho'^3 \\ & + 2gh\rho (g + \omega^2 \rho^2) (\Pi^2 + f^2 g \rho^2) \rho'' = 0. \end{aligned} \quad (3.14)$$

⁶Notice that dimensionless parameters were used in [17].

To solve the equation of motion, one should use the numerical tools.

The rotating-string solution starts at $u = 0, \rho = l$, passes through (u_c, ρ_c) and approaches the black hole horizon located at $u = u_h$ at a finite value of ρ that is greater than ρ_c which in turn is greater than l . By expanding (3.14) around u_c , one can find the series expansion of $\rho(u)$ as $\rho(u) = \rho(u_c) + (u - u_c)\rho'(u_c) + \frac{1}{2}(u - u_c)^2\rho''(u_c) + \dots$. For example, one finds that $\rho'(u_c)$ has four solutions

$$\begin{aligned} \rho_c^{(1,2)} &= \frac{1}{(4f_c g_c^3 \rho_c f_c')} \left[4f_c^2 g_c^3 h_c + g_c^3 \rho_c^2 f_c'^2 + \omega^2 g_c^2 \rho_c^4 f_c'^2 + 2f_c g_c^2 \rho_c^2 f_c' g_c' - \Pi^2 g_c'^2 \right. \\ &\quad \left. \pm \left(16f_c^2 g_c^6 h_c \rho_c^2 f_c'^2 + \left(4f_c^2 g_c^3 h_c + g_c^3 \rho_c^2 f_c'^2 + \omega^2 g_c^2 \rho_c^4 f_c'^2 + 2f_c g_c^2 \rho_c^2 f_c' g_c' - \Pi^2 g_c'^2 \right)^2 \right)^{1/2} \right], \\ \rho_c^{(3,4)} &= \pm \sqrt{-h_c}, \end{aligned} \tag{3.15}$$

Obviously, the 3rd and 4th solutions are not physical. The only acceptable solution is the 1st solution (positive sign) which leads to the physical behavior, $\rho(u = 0) = l < \rho_c$.⁷ Once we find the series expansion of $\rho(u)$ around u_c , it would be possible to guess the closed form of $\rho(u)$. In general it is not easy to find $\rho(u)$ in this way and the only known result is the simple case of rotating string at zero temperature $\mathcal{N} = 4$ SYM plasma in [29].⁸

We use numerical methods to find the shape of the rotating string. Given angular momentum ω and constant of motion Π , one finds (u_c, ρ_c) point from (3.7) and (3.8). But there is a problem at this point, the equation of motion (3.14) (and the Lagrangian (3.4)) is singular at this point so we can not find the solution numerically.⁹ Fortunately this problem appears only at one point and we can use the equation of motion (3.14) and expand it up to any order that we want. We can find the second derivative of the $\rho(u)$ at u_c , $\rho''(u_c)$ and then we can start finding the numerical solution by expanding from $u_c - \epsilon$ ($u_c + \epsilon$) to the boundary (horizon).

In general, the energy lost rate of the world-sheet is given by

$$\frac{dE}{dt} = \Pi_t^\sigma = -\frac{\delta S}{\delta(\partial_\sigma X^0)}, \tag{3.16}$$

In our case, by using equations (3.4), (3.5) and (3.9), one can show that there are different expansions for the rate of energy lost as,

$$\frac{dE}{dt} = -\frac{G_{tt} G_{\phi\phi} \omega \theta'}{2\pi\alpha' \mathcal{L}} = \frac{\Pi\omega}{2\pi\alpha'} = \frac{|G_{tt}(u_c)|}{2\pi\alpha'}. \tag{3.17}$$

In appendix A we will show that the general formula for the rate of energy lost for a string moves on a line is the same as the last equality in the above equation. The difference just comes from the different value for the critical holographic radial coordinate, u_c .

To find and investigate the solution in terms of the parameters of the boundary theory we will focus on the strongly coupled anisotropic plasma in the next section and compare our results with the rotating string in the isotropic background which is the $\text{AdS}_5 \times \text{S}^5$ theory with $\mathcal{N} = 4$ SYM theory on the boundary. Then we will compare the energy lost of a rotating string to the drag force in the strongly coupled anisotropic plasma studied in [23, 24] and the radiation results on isotropic case investigated in [17].

⁷Usually $f = u^n$ and it leads to a positive (negative) solution for ρ_c for $n > 0$ ($n < 0$).

⁸K.B.F thanks D.Nickel for discussion on this point.

⁹This problem have been seen in some other calculations [30] as well and it leads to using the Polyakov action instead of Nambu-Goto action.

4 Rotating string in strongly coupled anisotropic plasma

To find the energy lost of the rotating quark in strongly coupled anisotropic plasma, we only need to find the solution for the radius function $\rho(u)$. The general behavior of the angle function is the same as the isotropic case in [17], so we are not going to find the angle function $\theta(u)$.

The valuable results are the comparison of the anisotropic case with the isotropic background at the same temperature or at the same entropy density. So we will do these comparison both for the gravity side (bulk) and the field theory side (boundary) of the AdS/CFT correspondence.

By assumption the temperature and entropy density of the two sides of the AdS/CFT correspondence are the same then it's enough to find these parameters for the gravity side by using simple definitions of the temperature and entropy density.

Plugging anisotropic background (2.1) into the critical equations which determine the u_c and ρ_c values (3.9) the equation of motion for $\rho(u)$ (3.14) and the equation which determines the ρ'_c ; one can reduce the equations to the simpler form. As we mentioned in section 2 to find the numerical results for $\rho(u)$ we should start from $u_c - \epsilon$ ($u_c + \epsilon$) to the boundary (horizon).

In Fig.2. we compare the anisotropic plasma (lines) with isotropic plasma (dotted) with the same temperature. We have plotted the radial dependence $\rho(u)$ of spiraling string hanging down from rotating quarks for various different choices of parameters: $\omega = 0.05, \omega = 0.5$ and $\omega = 5.0$ from left to right. In this figure the constant of motion is given by $\Pi = 0.1$ (red), 1 (orange), 10 (blue), 100 (purple). The effect of anisotropic parameter is shown by $a/T \simeq 4.4$ and $a/T \simeq 86$ in (a) and (b), respectively. Note that the string is not going into the horizon so the dotted curves finished at the horizon of isotropic solutions.

We summarize the important results as follows

- The anisotropic parameter has a main effect on the the shape of spiraling string. One finds that by increasing this parameter the radius of rotation significantly changes.
- For the fixed ω and Π the radius on the boundary is bigger than the isotropic case which means the grater velocity of the quark at the field theory. Using the energy lost relation (3.17), $dE/dt \propto \Pi\omega$, one can show that for the same velocity v and the same angular velocity ω the energy lost in anisotropic plasma is less than isotropic case. we will discuss about this point in next sections.
- In the case of small ω (0.05) and any Π the larger anisotropy leads to the larger radius both at the horizon and on the boundary.
- for a bigger ω (0.5) the lines cross each other for enough large Π 's.
- In the case large ω (5.0), for small a/T the radius on the horizon is smaller than the isotropic case while,¹⁰ for large anisotropy the lines cross each other but the radius on the horizon is larger than isotropic case.
- The general behavior of the string for large a/T is almost the same for all of the ω 's and Π 's but, it is not the case for small a/T . In next sections we will discuss about this point which inherits from drag force results [23, 24].

¹⁰It is also the case for $\omega = 0.5$ and large enough Π 's.

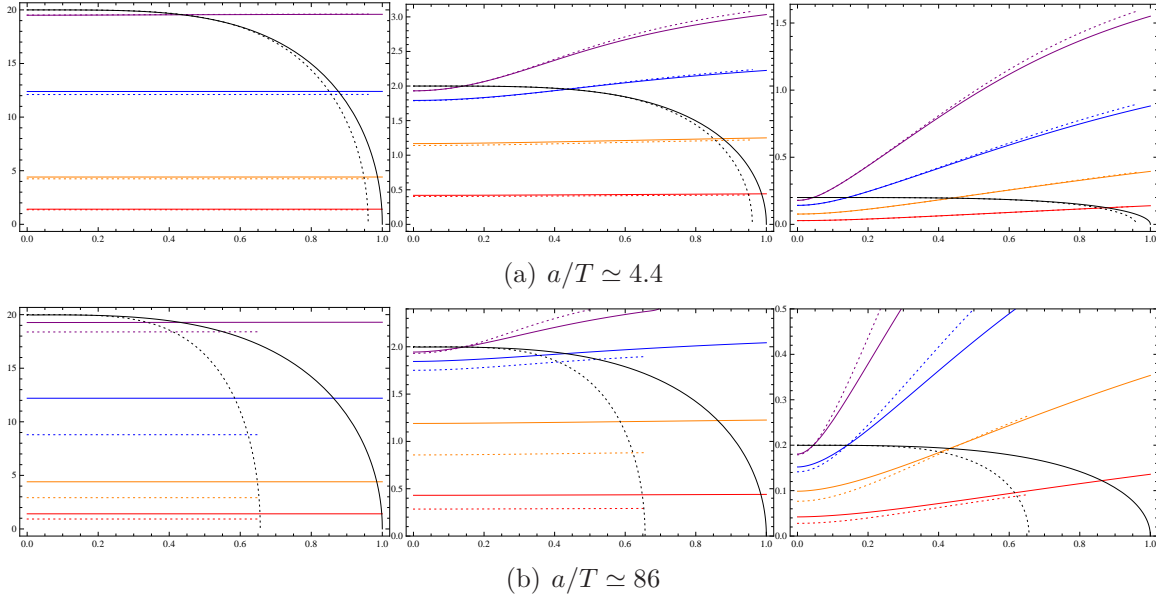


Figure 2: The radial dependence $\rho(u)$ of spiraling string hanging down from rotating quarks for various different choices of parameters: $\omega = 0.05, \omega = 0.5$ and $\omega = 5.0$ from left to right, and the set of values for the constant of motion $\Pi = 0.1$ (red), 1 (orange), 10 (blue), 100 (purple) for all of the figures. In (a) and (b), the anisotropic parameter is specified as $a/T \simeq 4.4$ and $a/T \simeq 86$, respectively. This comparison with the isotropic plasma has been done at the same temperature.

For the same entropy density one can show that the general behavior of the plots are the same as the plots we find for the same temperature cases. The main difference is for small a/T , there is no strange behavior as like as the same temperature cases we discussed early. This is very similar to the drag force results [23, 24]. We show the result in Fig. 3. Again, the anisotropic plasma plots showed by lines and the isotropic plasma showed by dotted, $\omega = 0.05, 0.5, 5.0$ from left to right and $\Pi = 0.1$ (red), 1 (orange), 10 (blue), 100 (purple). Here, one finds that the anisotropy leads to the bigger radius of the horizon at the same entropy.

It is obvious that the radius of the horizon for the isotropic background is smaller than the same temperature cases showed in figure 2. Comparing the same temperature case in figure 2 and the same entropy case in figure 3, one finds that, for the same ω and Π , the radius of rotating sting is smaller in the same entropy cases. Therefore, according to the general form of the rate of energy lost (3.17), the same value of the rate of energy lost in two different cases corresponded to the smaller velocity in the same entropy. Using the monotonic behavior of the velocity with respect to Π we conclude that with the same velocity the rate of energy lost for the same entropy is greater than for the same temperature cases which is in agreement with the numerical and analytical results we find in the next two sections.

4.1 The energy lost

In this section, we study energy lost of heavy test quark. Plugging the anisotropic background metric (2.1) into the general formula for the rate of energy lost (3.17) one can show

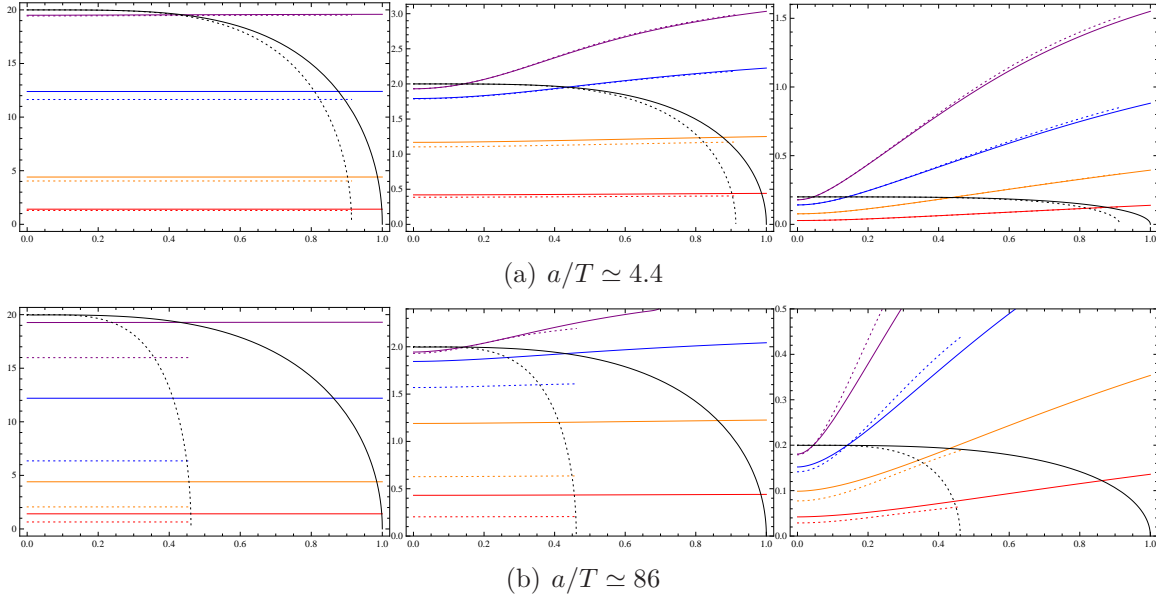


Figure 3: The radial dependence $\rho(u)$ of spiraling string hanging down from rotating quarks for various different choices of parameters: $\omega = 0.05, \omega = 0.5$ and $\omega = 5.0$ from left to right, and the set of values for the constant of motion $\Pi = 0.1$ (red), 1 (orange), 10 (blue), 100 (purple) for all of the figures. In (a) and (b), the anisotropic parameter is specified as $a/T \simeq 4.4$ and $a/T \simeq 86$, respectively. This comparison with the isotropic plasma has been done at the same entropy.

that it's given by

$$\frac{dE}{dt} = \frac{\Pi \omega}{2\pi\alpha'} = \frac{1}{2\pi\alpha'} \frac{\mathcal{F}_c \mathcal{B}_c}{u_c}, \quad (4.1)$$

where \mathcal{F}_c and \mathcal{B}_c are the value of these functions at the critical point (u_c, ρ_c) which is defined by

$$\frac{\mathcal{F}_c \mathcal{B}_c}{u_c^2} = \Pi \omega, \quad \rho_c = u_c \sqrt{\frac{\Pi}{\omega}} \quad (4.2)$$

Therefore, from gravity point of view, the energy lost just depends on the value of u_c which is a function of Π and ω through the equation (4.2).

The result (4.1) makes it straightforward to use the numerical calculations described before to evaluate the energy loss for a quark moving in a circle with angular frequency ω as a function of the radius of the circle l (or equivalently as a function of velocity of the quark which is $v = l\omega$). We pick ω and a series of values of Π . For each Π , we obtain the corresponding string world-sheet. From that solution, one finds that energy loss of quark increases without bound as l approaches $1/\omega$, which is the radius at which the quark would be moving at the speed of light. We call the radius of the rotating quark in the anisotropic and isotropic medium as l_{an} and l_{is} , respectively. In Fig.4 we plot the velocity of the quark in terms of the Π for $\omega = 5.0$ and $a/T \simeq 86$. This behavior is general for any value of ω and a/T . The main important feature of this plot is the velocity of the quark (radius of rotation) is a monotonic function of Π . It will be extremely useful for our discussions in next sections.

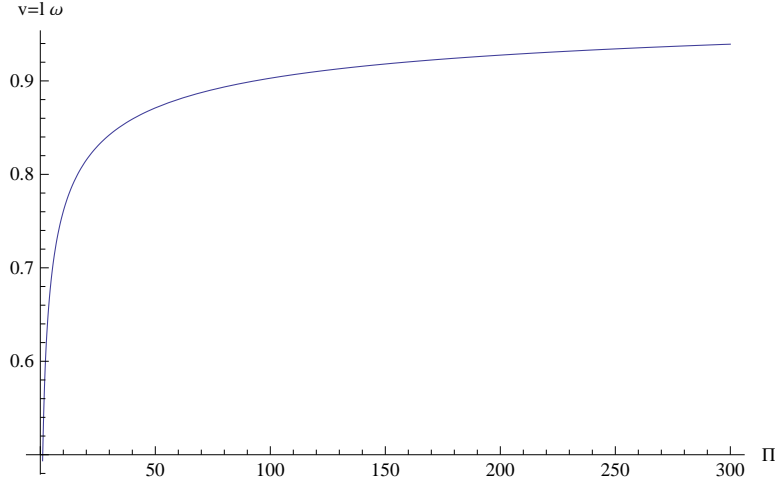


Figure 4: The velocity of the quark at the boundary versus the constant of motion Π for $\omega = 5.0$ and $a/T \simeq 86$.

In Fig. 5 we plot l_{an}/l_{is} as a function of the constant of motion Π . In each plot of this figure, angular velocity is $\omega = 0.05$ (red), 0.5 (green), 5.0 (black). From left to right the anisotropic parameter increases as $a/T = 0.78, 24.92, 86$.

It is clearly seen that for the same temperature cases, there is a minimum value for this ratio in the case of $\omega = 0.05$ and small $a/T (\simeq 0.78)$. This minimum disappear by increasing the angular velocity and/or a/T . All plots with same entropy in second row of Fig.5 show that l_{an} is bigger than l_{is} .

To compare the energy lost in two different medium it is natural to keep the velocity, $v = l\omega$ and angular velocity ω fixed. On the other hand, according to the first equality in equation (4.1), the energy lost rate is proportional to $\Pi\omega$. As we can see in Fig.5 in both isotropic and anisotropic cases the radiuses of rotation at the boundary are monotonically increasing with respect to Π . Therefor for $l_{an}/l_{is} > 1 (< 1)$ the rate of energy lost in anisotropic plasma is smaller (larger) than the isotropic case, for the fixed v and ω . It is easy to see that in these conditions the rate of energy lost in anisotropic plasma is less than isotropic case in general except for the small value of $\omega(0.05)$ and small $a/T (\simeq 0.78)$. In this case for large enough $\Pi (\gtrsim 40)$, corresponded to $v \simeq 0.9$, the energy loss rate in anisotropic plasma is more than isotropic case. This is in perfect agreement with drag force results [23, 24]. Naturally, we expect that for small angular velocity ω the dominant part of the energy lost is drag force, and the above agreement justify this idea definitely. We checked this behavior for a range a/T and we see that this happens for $a/T \lesssim 12$.

Another interesting point about Fig.5 is for the larger Π (which leads to larger quark velocity) the ratio of energy loss rate is going to 1 for all of the value of ω and a/T . It shows that the ultrarelativistic quark can not see the anisotropy in terms of its energy lost rate while, we will see in next sections that each part of energy lost, linear and radiation, behaves differently.

It would be very interesting to ask about mechanism of energy loss in two plasmas, is it drag force or radiation? In section 6 we will show that the anisotropy decreases the radiation when the parton propagates perpendicular to the direction of the anisotropy. This is in perfect agreement with result of [31]. We will discuss on this result later.

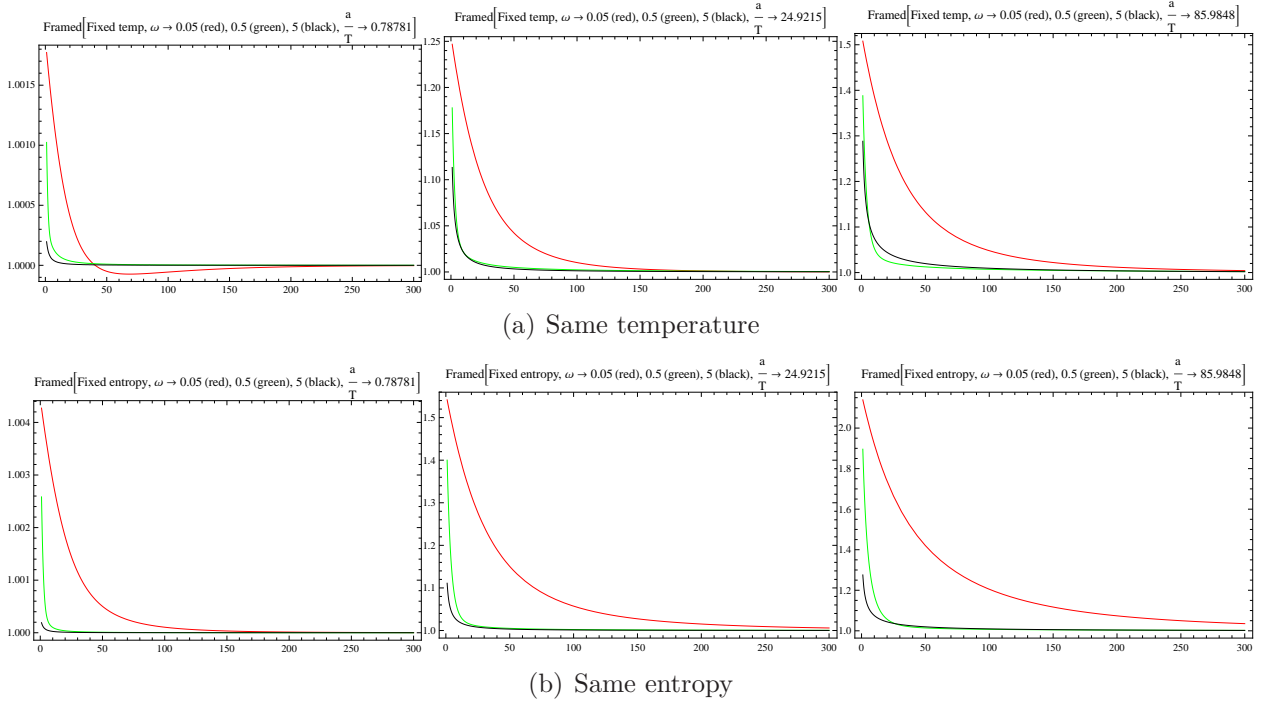


Figure 5: The ratio of the radius of rotating quark in an anisotropic medium to the isotropic case as a function of the constant of motion Π . This comparison has been done for the same temperature and entropy in (a) and (b), respectively. In each plot of this figure, angular velocity is $\omega = 0.05$ (red), 0.5 (green), 5.0 (black). From left to right $a/T \simeq 0.78, 24.92, 86$.

5 Analytic limits

In this section, we consider two different limits, ultra-relativistic limit and small a/T limit. For these cases we know the metric functions of dual gravity (2.1) explicitly [20] and we can do some analytic calculations to justify our numeric results at least in these limits. The results also show that the energy loss rate depend on the temperature (or horizon radius) and a/T .

5.1 Ultra-relativistic limit

There are two different options for ultra-relativistic limit,

- Large but fixed $v = l\omega = \text{const.}$, $a = v\omega \rightarrow 0$, meaning $\omega \rightarrow 0$
- Large but fixed $v = l\omega = \text{const.}$, $a = v\omega \rightarrow \infty$, meaning $\omega \rightarrow \infty$

For the second case as we see in Fig.2 and Fig.3 that the critical point u_c can be anywhere between the horizon $u = u_h$ and the boundary $u = 0$. For this case which is completely general we know nothing analytically. But for the first case, as like as drag force, in the large velocity limit $v \rightarrow 1$ the critical point u_c approaches to the boundary

$u_c \rightarrow 0$.¹¹ Therefore one can use the near boundary expansion of metric functions [20],

$$\begin{aligned}\mathcal{F} &= 1 + \frac{11a^2}{24}u^2 + \left(\mathcal{F}_4 + \frac{7a^4}{12}\log u\right)u^4 + \mathcal{O}(u^6), \\ \mathcal{H} &= 1 + \frac{a^2}{4}u^2 - \left(\frac{2\mathcal{B}_4}{7} - \frac{5a^4}{4032} - \frac{a^4}{6}\log u\right)u^4 + \mathcal{O}(u^6), \\ \mathcal{B} &= 1 - \frac{11a^2}{24}u^2 + \left(\mathcal{B}_4 - \frac{7a^4}{12}\log u\right)u^4 + \mathcal{O}(u^6),\end{aligned}\tag{5.1}$$

where \mathcal{F}_4 and \mathcal{B}_4 depend on a , T and a conformal anomaly scale and, they are not determined by the near boundary analysis [20].

To find the critical point (u_c, ρ_c) for this case, we solve the equations (4.2) analytically for the above expansion of metric functions. The second equation in (4.2) is simplified to

$$\Pi\omega = \frac{v_c^2}{u_c^2},\tag{5.2}$$

where $v_c = \rho_c \omega$ is the velocity of the string at the critical point, u_c . Note that in this limit the radius of the rotating string at the boundary, l , is very close to the radius of the string at the critical point, ρ_c and the velocity of the string at these two points are also very close to each other. So we can find the value of u_c by solving the first equation in (4.2) to leading order in $1 - v_c^2$ which is

$$\frac{1}{u_c^2} = \frac{T^2}{\sqrt{1 - v_c^2}}A, \quad A = \sqrt{\frac{121a^4}{576T^4} - \frac{\mathcal{F}_4 + \mathcal{B}_4}{T^4}}\tag{5.3}$$

which is the same expansion for the critical point found for drag force calculation [23]. But we should remind that v_c is a function of u_c , (5.2) so the explicit relation for u_c is given by

$$u_c = \frac{1}{AT^2} \sqrt{-\frac{\Pi\omega}{2} + \frac{1}{2}\sqrt{\Pi^2\omega^2 + 4A^2T^4}},\tag{5.4}$$

Remind that the energy lost rate is given by the value of time component of the background metric at the critical point, $|G_{tt}(u_c)|$, (3.17),

$$\frac{dE}{dt}|_{aniso} = \frac{\sqrt{\lambda}T^2}{2\pi} \frac{v_c^2}{\sqrt{1 - v_c^2}} \sqrt{\frac{121a^4}{576T^4} - \frac{\mathcal{F}_4 + \mathcal{B}_4}{T^4}}.\tag{5.5}$$

Again, this is exactly the same results which was found for the linear drag in [23] and we will explain in the next section.

For the linear drag there is only one velocity for all of the points of string but in our case the velocity is the velocity of the critical point of the string, v_c . As it is shown in Fig.6 for small enough Π (which corresponded to small enough radius of rotation at the boundary, l) at $\omega = 0.05$ and $\omega = 0.5$ the rate of energy lost is described by linear dragging. But the validity for this description is not just $a \rightarrow 0$, because for large Π (l) one can see from Fig.2 and Fig.3 that despite the radius (velocity) of rotating string at the boundary, $u = 0$, and

¹¹From Fig.2 and Fig.3, it is easy to see that for fixed ω , the larger velocity corresponded to larger radius of rotation at the boundary which leads to larger Π . And obviously it guides to the small value of u_c .

critical point, $u = u_c$, are the same as the rest of the string below the critical point has larger radius (velocity). So the $v \simeq v_c$ approximation is not valid any more. This is the limit which is discussed in [17] for the validity in isotropic case as well.

Since the the energy lost rate (5.5) is the same as the linear dragging [23] and its validity range is as same as isotropic the case, we can easily find that the comparison between the energy lost rate in anisotropic and isotropic backgrounds leads to the same results for the drag force. Remind that this is true just in special limit which is: large but fixed $v = l\omega = \text{const.}$, $\omega \rightarrow 0$ and small enough l .

For small and large a/T limits the \mathcal{F}_4 and \mathcal{B}_4 parameters are known [20] and one can find explicit results. In small a/T

$$\begin{aligned}\mathcal{F}_4 &= -\pi^4 T^4 - \frac{9\pi^2 T^2}{16} a^2 - \left[\frac{101}{384} - \frac{7}{12} \log\left(\frac{2\pi T}{a}\right) - \frac{7}{12} \log\left(\frac{a}{\Lambda}\right) \right] a^4 + \mathcal{O}(a^6), \\ \mathcal{B}_4 &= \frac{7\pi^2 T^2}{16} a^2 + \left[\frac{593}{1152} - \frac{7}{12} \log\left(\frac{2\pi T}{a}\right) - \frac{7}{12} \log\left(\frac{a}{\Lambda}\right) \right] a^4 + \mathcal{O}(a^6),\end{aligned}\quad (5.6)$$

where Λ relates to the conformal anomaly scale. Since, only the sum of \mathcal{F}_4 and \mathcal{B}_4 appears in (5.5), the ratio of energy losses doesn't depend to parameter Λ . For the same temperature case one can show that ratio of the energy lost rates is given by

$$\frac{dE/dt_{aniso}}{dE/dt_{iso}} \Big|_{\text{temp}} = 1 + \frac{a^2}{16\pi^2 T^2} + \mathcal{O}\left(\frac{a^4}{T^4}\right). \quad (5.7)$$

Therefore as like as drag force calculation the energy lost rate on ultra-relativistic quark moving on a circle in transverse direction plane in an anisotropic plasma with small a/T , small ω and small enough l is greater than the isotropic case at the same temperature. These results are in agreement with our numerical results in Fig. 6.

To compare the results for the same entropy density, we should use the relation between entropy density and temperature for an anisotropic plasma in small a/T which is given by [20]

$$s = \frac{\pi^2 N_c^2 T^3}{2} + \frac{N_c^2 T}{16} a^2 + \mathcal{O}\left(\frac{a^4}{T^4}\right), \quad (5.8)$$

which leads to different ratio for the rate of energy lost,

$$\frac{dE/dt_{aniso}}{dE/dt_{iso}} \Big|_{\text{entropy}} = 1 - \frac{N_c^{4/3}}{48(2\pi)^{3/2}} \left(\frac{a}{s^{1/3}}\right)^2 + \mathcal{O}\left(\frac{a^4}{s^{4/3}}\right). \quad (5.9)$$

Again, it is similar to the drag force and the energy lost rate in the anisotropic plasma is smaller than the isotropic case at the same entropy density. These results are in agreement with our numerical results in Fig.6 as well.

In large a/T , one can show easily that the results are the same as the linear drag, as one expected, and the rate of energy lost in the anisotropic plasma is always greater than the isotropic case both for the same temperature and the same entropy density. Using the explicit relations for \mathcal{F}_4 and \mathcal{B}_4 parameters given in [20] the ratio of energy loss rates are given by

$$\frac{dE/dt_{aniso}}{dE/dt_{iso}} \Big|_{\text{temp}} = \frac{\sqrt{2c_{\text{ent}}}}{\pi} \left(\frac{a}{T}\right)^{1/3} + \dots, \quad (5.10)$$

$$\frac{dE/dt_{aniso}}{dE/dt_{iso}} \Big|_{\text{entropy}} = \frac{1}{2^{1/6} \pi^{1/3} c_{\text{ent}}^{3/16} N_c^{1/24}} \left(\frac{s^{1/3}}{a}\right)^{1/16} + \dots, \quad (5.11)$$

for the same temperature and the same entropy cases. c_{ent} is a constant introduced in the entropy density in section 2.

5.2 Small a/T limit

For small a/T the metric functions and the radius of the horizon are known [20],

$$\mathcal{F} = 1 - \frac{u^4}{u_H^4} + a^2 \mathcal{F}_2 + \mathcal{O}(a^4), \quad (5.12)$$

$$\mathcal{B} = 1 + a^2 \mathcal{B}_2 + \mathcal{O}(a^4), \quad (5.13)$$

$$\log \mathcal{H} = \frac{a^2 u_H^2}{4} \log \left(1 + \frac{u^2}{u_H^2} \right) + \mathcal{O}(a^4), \quad (5.14)$$

$$u_H = \frac{1}{\pi T} + \frac{5 \log 2 - 2}{48 \pi^3 T^3} a^2 + \mathcal{O}(a^4), \quad (5.15)$$

in which

$$\mathcal{F}_2 = \frac{1}{24 u_H^2} \left[8u^2(u_H^2 - u^2) - 10u^4 \log 2 + 3u_H^4 + 7 \log \left(1 + \frac{u^2}{u_H^2} \right) \right], \quad (5.16)$$

$$\mathcal{B}_2 = -\frac{u_H^2}{24} \left[\frac{10u^2}{u_H^2 + u^2} + \log \left(1 + \frac{u^2}{u_H^2} \right) \right]. \quad (5.17)$$

Now we can find the critical point by using the general formula (3.9). Obviously the result is the critical point for isotropic case (3.11) with a correction in a leading order (a^2/T^2),

$$u_c = u_{\text{iso}} + a^2 u_{c;2} + \mathcal{O}(a^4), \quad \rho_c = u_c \sqrt{\frac{\Pi}{\omega}}, \quad (5.18)$$

where

$$u_{\text{iso}} = \frac{1}{\pi^2 T^2} \sqrt{-\frac{\Pi \omega}{2} + \frac{1}{2} \sqrt{\Pi^2 \omega^2 + 4\pi^4 T^4}},$$

$$u_{c;2} = \frac{3 - 2\pi^2 T^2 u_{\text{iso}}^2 (1 + \pi^2 T^2 u_{\text{iso}}^2) + (-1 + 8\pi^4 T^4 u_{\text{iso}}^4) \log(1 + \pi^2 T^2 u_{\text{iso}}^2)}{48\pi^2 T^2 u_{\text{iso}} (2\pi^4 T^4 u_{\text{iso}}^2 + \Pi \omega)}. \quad (5.19)$$

To explain every thing from boundary theory point of view we should find a numerical result for $\rho(u)$ by plugging the above results to the metric functions and in the general equation of motion for ρ (3.14). It is easy to show that the results are in perfect agreement with the results we found generally for small a/T in previous sections.

6 Comparison with linear drag and synchrotron radiation

In this section we compare our results for the rate of energy lost with two different known cases, the linear drag and synchrotron radiation, with the same velocity.

First we want to compare energy loss rate of rotating quark with linear drag. The drag force experienced by an infinitely massive quark propagating at constant velocity through

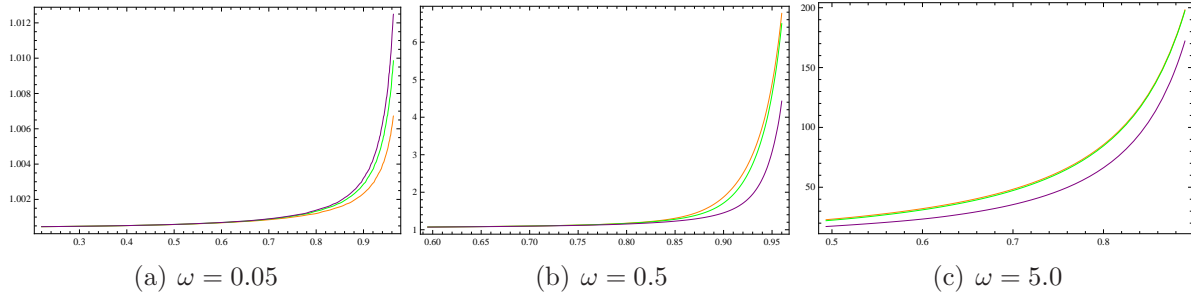


Figure 6: The ratio of the rate of energy lost to the linear drag. $a/T=1.4$ (orange), 12.2 (green), 86 (purple)

an anisotropic, strongly coupled $\mathcal{N} = 4$ plasma was calculated in [23, 24]. In Fig.6 we show the ratio of energy loss rate of rotating quark to its dragging part in terms of velocity of the quark on the boundary for different ω 's a/T .

As we expected, for small ω the dominant part of the ratio of energy lost is the linear drag for a wide range of velocity of the quark on the boundary. It is because, in this range, the local velocity of the rotating string at each point is close to the velocity of the quark at the boundary and so, the string behaves similar to the linear drag case which is studied in [23, 24].

In this limit we can show a perfect agreement between the energy loss rate of rotating quark and straight moving quark analytically. The rate of energy lost for a rotating string is given by (3.17),

$$\frac{dE}{dt} = \frac{\Pi\omega}{2\pi\alpha'} = \frac{\Pi v_c}{2\pi\alpha' l}. \quad (6.1)$$

Note that in this limit the velocity of string is close to v_c for all of the points. Using the general relations between rotation and linear motion, assumption of constant velocity at each point of the rotating string and equation (A.8) lead to

$$\frac{dE}{dt} = \frac{\mathcal{P}v}{2\pi\alpha'} = \frac{dE^{(\text{drag})}}{dt}. \quad (6.2)$$

This result is broken for ultra-relativistic quark since the radius (velocity) of the rotation is getting larger from ρ_c for $u_c > u \geq u_H$, $\rho(u) > \rho_c$, and so the constant constant for all of the string's points is not good approximation.

It is easy to see that for larger ω 's the the range of velocity in which the dominant part of the rate of energy lost is the dragging would be smaller. There is another point we would like to emphasis. The ratio of the rate of energy lost through rotation to linear drag for small ω , for smaller a/T is closer to 1. But for large ω , the bigger a/T is more close to 1. At this stage we do not have any explanation for this phenomena.

In [17] it was shown that for large ω the energy lost through radiation channel is dominant. They showed this result by comparing the energy lost with the synchrotron radiation introduced by Mikhailov [32]. Therefor, to compare the rate of energy lost with the synchrotron radiation we use the Mikhailov's formula for the radiation of quark in vacuum,

$$\frac{dE}{dt} \Big|_{\text{vacuum radiation}} = \frac{\sqrt{\lambda}}{2\pi} \frac{v^2\omega^2}{(1-v^2)^2}. \quad (6.3)$$

The ratio of the rate of energy lost to the above rate is actually the ratio of energy loss to the radiation in isotropic plasma. The results are given in Fig.7. For small ω one

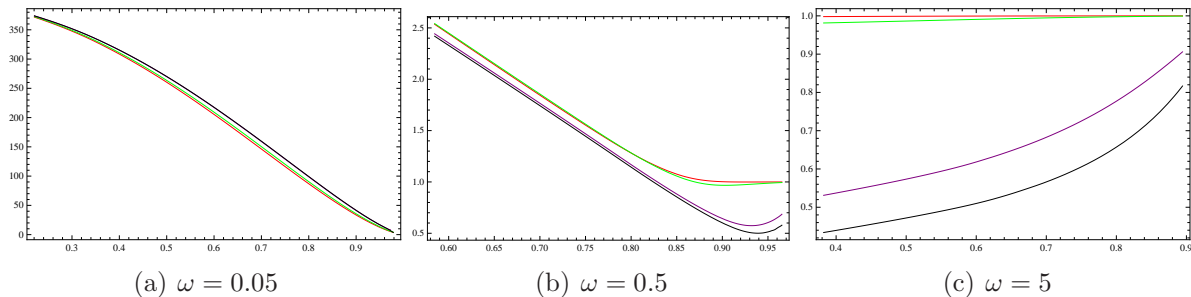


Figure 7: The ratio of the rate of energy lost to the radiation. $a/T=0.8$ (red)4.4(green), 54(purple), 86(black)

can see that the total energy loss rate is much much more than radiation part which is in agreement with the results we find in Fig.6 (that the dominant part of the energy loss is linear drag). For large ω which the dominant part of energy lost is radiation one can see that the radiation in anisotropic plasma is less than isotropic case and the larger a/T , leads to smaller radiation. But for ultra-relativistic quarks the radiation is close to isotropic case which means ultra-relativistic quarks can not see the anisotropy in terms of the energy loss through radiation channel.

7 Summary and discussion

In this paper, we have studied the energy loss of a rotating heavy quark in a strongly coupled anisotropic plasma from holography. There are two models to investigate anisotropic plasma from AdS/CFT correspondence which have been proposed in [20, 33]. In the model by Janik and Witaszczyk [33], a geometry involving a comparatively benign naked singularity was considered, while Mateos and Trancanelli [20] have introduced a regular geometry involving a nontrivial axion field dual to a parity-odd deformation of the gauge theory. Different aspects of these models have been studied in [34]. The latter model has been used in this paper. In this model, the anisotropic $\mathcal{N} = 4$ SYM plasma is symmetric in xy plane but in the beam direction (z direction) is not. Then in the context of heavy ion collisions, we have considered rotating test quark within the transverse plane which is also mostly interested in jets at this plane.

Holographic study of the momentum broadening in the anisotropic medium shows that this quantity along the beam axis and along the transverse plane will generically differ [23, 24, 25]. These quantities in a weakly coupled anisotropic plasma have been studied in [35, 36, 37]. They found that the momentum broadening along the beam axis increases slightly in the presence of anisotropy, whereas the momentum broadening in the transverse plane decreases more significantly. Especially, the jet quenching parameter was studied in [24, 25, 34] and it was found that for large anisotropic parameter the same result can be achieved. We have seen that in the regime where we expect to see the radiation of beam of synchrotron-like radiation, the energy loss is significantly less than the isotropic case.

It would be interesting to compare our results with the radiative energy loss of heavy quarks in a real anisotropic plasma. This study in a first-order opacity expansion has been done in [31]. It was found that the radiation energy loss depends on the direction of propagation of the fast partons with respect to the anisotropy axis as well as on the

anisotropy parameter. It was shown that in the direction parallel to the anisotropy direction radiation increases while in the transverse direction it decreases. Regarding our setup, we have considered the radiation in the transverse plane and found that radiation in a strongly coupled anisotropic plasma is less than the isotropic case.

The energy density and angular distribution of the power radiated by a rotating quark in a strongly coupled isotropic plasma was studied in [29]. This study was also extended to the case of non-zero temperature in [40]. It would be interesting to study effect of anisotropic parameter on the angular distribution of the power radiated by heavy quark through the anisotropic plasma. One can find from our study that the crossover from the drag-dominated regime to the radiation-dominated regime significantly depends on the anisotropic parameter. It was found that unlike in vacuum, in the plasma at nonzero temperature the energy disturbance created by the rotating quark can excite two qualitatively distinct modes in the energy density; a sound mode and a light-like mode which propagates at the speed of light. The energy loss due to unstable modes in a weakly coupled anisotropic plasma has been studied in [38, 39]. It would be very interesting to understand the effect of instability modes on the energy density. This calculation can be shed new light to the similarities between the quenching of the beam of strongly coupled synchrotron radiation in the strongly coupled anisotropic $\mathcal{N} = 4$ SYM plasma and the quenching of jets in heavy ion collisions at the LHC and RHIC.

Acknowledgements

We would like to thank M. Ali-Akbari, N. Abbasi, A. Davody, M. Abedini, E. Azimfarid, D. Giataganas, K. Goldstein, D. Nickel and M. M. Sheikh-jabbari for useful discussions on the different aspects of rotating string in an anisotropic background. K. B. F. thanks a lot from M. Strickland for discussion on the papers in the subject of weakly anisotropic plasma. H. S. thanks R. Warmbier and R. Morad for their comments on numerical calculations. H. S. would like to thank Institute for Research in Fundamental Sciences (IPM) for hospitality during different stages of preparing this project. H. S. is supported by National Research Foundation (NRF). Any opinion, findings and conclusions or recommendations expressed in this material are those of the H. S. and therefore the NRF do not accept any liability with regard thereto.

A Linear drag in a general background

In this appendix we want to give a fast review on a linear drag case corresponded to a quark moving in a straight line with a fixed speed v in a general background which has been known for some especial examples [12]. Using the static gauge for a string moves in x direction of a general background (3.1)

$$X_{\text{drag}}^\mu(\tau, \sigma) = (t = \tau, u = \sigma, x = \xi(u) + vt, y = z = 0), \quad (\text{A.1})$$

one can show that the Nambu-Goto action is given by the following density of lagrangian

$$\mathcal{L}_{\text{drag}} = [-G_{tt}G_{uu} - G_{xx}G_{tt}\xi'^2 - G_{xx}G_{uu}v^2]^{1/2}. \quad (\text{A.2})$$

Since ξ does not appear explicitly in the action, its momentum conjugate is conserved and the equation of motion is given by

$$\mathcal{P} = \frac{\partial \mathcal{L}}{\partial \xi'} = -\frac{G_{tt}G_{xx}\xi'}{\mathcal{L}} = \text{constant}. \quad (\text{A.3})$$

Solving this equation for ξ' yields

$$\xi'^2 = -\mathcal{P}^2 \frac{G_{uu}(G_{tt} + G_{xx}v^2)}{G_{xx}G_{tt}(G_{xx}G_{tt} + \mathcal{P}^2)}. \quad (\text{A.4})$$

The positivity of LHS leads to the fact that there is a critical point, $u_c^{(\text{drag})}$, that both numerator and denominator change the sign which is defined by

$$G_{tt}(u_c)^{(\text{drag})} + G_{xx}(u_c)^{(\text{drag})}v^2 = 0, \quad (\text{A.5})$$

$$G_{xx}(u_c)^{(\text{drag})} G_{tt}(u_c)^{(\text{drag})} + \mathcal{P}^2 = 0, \quad (\text{A.6})$$

which lead to

$$|G_{tt}(u_c)^{(\text{drag})}| = \mathcal{P}v, \quad G_{xx}(u_c)^{(\text{drag})} = \frac{\mathcal{P}}{v}. \quad (\text{A.7})$$

On the other hand, by using (A.5) and (A.6), it is easy to show that the rate of energy lost according to draggening of moving string is given by

$$\frac{dE^{(\text{drag})}}{dt} = \Pi_t^{\sigma(\text{drag})} = \frac{\mathcal{P}v}{2\pi\alpha'} = \frac{|G_{tt}(u_c)^{(\text{drag})}|}{2\pi\alpha'}, \quad (\text{A.8})$$

where in the second equality we used the first equation in (A.7). Comparing equations (3.17) and (A.8) shows that the general form of the rate of energy lost in both linear and rotating strings are the same and it's just a function of critical point.

Therefore, if the value of critical point at two different cases are the same the rate of energy lost should be the same. As we show in section 5.1 for small angular velocity the value of critical point is close to the linear drag both numerically and analytically.

References

- [1] J. Casalderrey-Solana, H. Liu, D. Mateos, K. Rajagopal and U. A. Wiedemann, "Gauge/String Duality, Hot QCD and Heavy Ion Collisions," arXiv:1101.0618 [hep-th].
- [2] The ALICE Collaboration, K. Aamodt et al., "Elliptic flow of charged particles in Pb-Pb collisions at 2.76 TeV," arXiv:1011.3914 [nucl-ex].
- [3] P. Romatschke and M. Strickland, "Collective modes of an anisotropic quark gluon plasma," Phys. Rev. D **68** (2003) 036004 [hep-ph/0304092].
- [4] P. B. Arnold, G. D. Moore and L. G. Yaffe, "The Fate of non-Abelian plasma instabilities in 3+1 dimensions," Phys. Rev. D **72** (2005) 054003 [hep-ph/0505212].
- [5] A. Rebhan, M. Strickland and M. Attems, "Instabilities of an anisotropically expanding non-Abelian plasma: 1D+3V discretized hard-loop simulations," Phys. Rev. D **78** (2008) 045023 [arXiv:0802.1714 [hep-ph]].
- [6] J. M. Maldacena, "The large N limit of superconformal field theories and supergravity," Adv. Theor. Math. Phys. **2** (1998) 231 [Int. J. Theor. Phys. **38** (1999) 1113] [arXiv:hep-th/9711200].

- [7] S. S. Gubser, I. R. Klebanov and A. M. Polyakov, “Gauge theory correlators from non-critical string theory,” *Phys. Lett. B* **428** (1998) 105 [arXiv:hep-th/9802109].
- [8] E. Witten, “Anti-de Sitter space and holography,” *Adv. Theor. Math. Phys.* **2** (1998) 253 [arXiv:hep-th/9802150].
- [9] E. Witten, “Anti-de Sitter space, thermal phase transition, and confinement in gauge theories,” *Adv. Theor. Math. Phys.* **2** (1998) 505 [arXiv:hep-th/9803131].
- [10] H. Liu, K. Rajagopal and U. A. Wiedemann, “Calculating the jet quenching parameter from AdS/CFT,” *Phys. Rev. Lett.* **97** (2006) 182301 [hep-ph/0605178].
- [11] C. P. Herzog, A. Karch, P. Kovtun, C. Kozcaz and L. G. Yaffe, “Energy loss of a heavy quark moving through N=4 supersymmetric Yang-Mills plasma,” *JHEP* **0607** (2006) 013 [arXiv:hep-th/0605158].
- [12] S. S. Gubser, “Drag force in AdS/CFT,” *Phys. Rev. D* **74** (2006) 126005 [arXiv:hep-th/0605182].
- [13] S. S. Gubser, S. S. Pufu, F. D. Rocha and A. Yarom, “Energy loss in a strongly coupled thermal medium and the gauge-string duality,” arXiv:0902.4041 [hep-th];
M. Chernicoff, J. A. Garcia, A. Guijosa and J. F. Pedraza, “Holographic Lessons for Quark Dynamics,” *J. Phys. G G* **39** (2012) 054002 [arXiv:1111.0872 [hep-th]];
N. Abbasi and A. Davody, “Moving Quark in a Viscous Fluid,” arXiv:1202.2737 [hep-th];
K. B. Fadafan, “Charge effect and finite ’t Hooft coupling correction on drag force and Jet Quenching Parameter,” *Eur. Phys. J. C* **68** (2010) 505 [arXiv:0809.1336 [hep-th]];
K. B. Fadafan, “R**2 curvature-squared corrections on drag force,” *JHEP* **0812** (2008) 051 [arXiv:0803.2777 [hep-th]];
J. Sadeghi and B. Pourhassan, “STU/QCD Correspondence,” arXiv:1205.4254 [hep-th].
- [14] F. Dominguez, C. Marquet, A. H. Mueller, B. Wu and B. -W. Xiao, “Comparing energy loss and p-perpendicular - broadening in perturbative QCD with strong coupling N = 4 SYM theory,” *Nucl. Phys. A* **811** (2008) 197 [arXiv:0803.3234 [nucl-th]].
- [15] M. Chernicoff and A. Guijosa, “Acceleration, Energy Loss and Screening in Strongly-Coupled Gauge Theories,” *JHEP* **0806** (2008) 005 [arXiv:0803.3070 [hep-th]].
- [16] Y. Hatta, E. Iancu, A. H. Mueller and D. N. Triantafyllopoulos, “Radiation by a heavy quark in N=4 SYM at strong coupling,” *Nucl. Phys. B* **850** (2011) 31 [arXiv:1102.0232 [hep-th]].
- [17] K. B. Fadafan, H. Liu, K. Rajagopal and U. A. Wiedemann, “Stirring Strongly Coupled Plasma,” *Eur. Phys. J. C* **61** (2009) 553 [arXiv:0809.2869 [hep-ph]].
- [18] M. Ali-Akbari and U. Gursoy, “Rotating strings and energy loss in non-conformal holography,” *JHEP* **1201** (2012) 105 [arXiv:1110.5881 [hep-th]].
- [19] E. Kiritsis and G. Pavlopoulos, “Heavy quarks in a magnetic field,” *JHEP* **1204** (2012) 096 [arXiv:1111.0314 [hep-th]].

- [20] D. Mateos and D. Trancanelli, “The anisotropic $N=4$ super Yang-Mills plasma and its instabilities,” *Phys. Rev. Lett.* **107** (2011) 101601 [arXiv:1105.3472 [hep-th]];
D. Mateos and D. Trancanelli, “Thermodynamics and Instabilities of a Strongly Coupled Anisotropic Plasma,” *JHEP* **1107** (2011) 054 [arXiv:1106.1637 [hep-th]].
- [21] T. Azeyanagi, W. Li and T. Takayanagi, “On String Theory Duals of Lifshitz-like Fixed Points,” *JHEP* **0906** (2009) 084 [arXiv:0905.0688 [hep-th]].
- [22] K. B. Fadafan, “Drag force in asymptotically Lifshitz spacetimes,” arXiv:0912.4873 [hep-th].
- [23] M. Chernicoff, D. Fernandez, D. Mateos and D. Trancanelli, “Drag force in a strongly coupled anisotropic plasma,” arXiv:1202.3696 [hep-th].
- [24] D. Giataganas, “Probing strongly coupled anisotropic plasma,” arXiv:1202.4436 [hep-th].
- [25] M. Chernicoff, D. Fernandez, D. Mateos and D. Trancanelli, “Jet quenching in a strongly coupled anisotropic plasma,” arXiv:1203.0561 [hep-th].
- [26] A. Rebhan and D. Steineder, “Violation of the Holographic Viscosity Bound in a Strongly Coupled Anisotropic Plasma,” *Phys. Rev. Lett.* **108** (2012) 021601 [arXiv:1110.6825 [hep-th]].
- [27] P. Kovtun, D. T. Son and A. O. Starinets, “Viscosity in strongly interacting quantum field theories from black hole physics,” *Phys. Rev. Lett.* **94** (2005) 111601 [hep-th/0405231].
- [28] M. Brigante, H. Liu, R. C. Myers, S. Shenker and S. Yaida, “The Viscosity Bound and Causality Violation,” *Phys. Rev. Lett.* **100** (2008) 191601 [arXiv:0802.3318 [hep-th]];
Y. Kats and P. Petrov, “Effect of curvature squared corrections in AdS on the viscosity of the dual gauge theory,” *JHEP* **0901** (2009) 044 [arXiv:0712.0743 [hep-th]].
- [29] C. Athanasiou, P. M. Chesler, H. Liu, D. Nickel and K. Rajagopal, “Synchrotron radiation in strongly coupled conformal field theories,” *Phys. Rev. D* **81** (2010) 126001 [Erratum-ibid. *D* **84** (2011) 069901] [arXiv:1001.3880 [hep-th]].
- [30] P. M. Chesler, K. Jensen, A. Karch and L. G. Yaffe, “Light quark energy loss in strongly-coupled $N = 4$ supersymmetric Yang-Mills plasma,” *Phys. Rev. D* **79** (2009) 125015 [arXiv:0810.1985 [hep-th]].
- [31] P. Roy and A. K. Dutt-Mazumder, “Radiative energy loss in an anisotropic Quark-Gluon-Plasma,” *Phys. Rev. C* **83** (2011) 044904 [arXiv:1009.2304 [nucl-th]].
- [32] A. Mikhailov, “Nonlinear waves in AdS / CFT correspondence,” hep-th/0305196.
- [33] R. A. Janik and P. Witaszczyk, “Towards the description of anisotropic plasma at strong coupling,” *JHEP* **0809** (2008) 026 [arXiv:0806.2141 [hep-th]].
- [34] A. Rebhan and D. Steineder, “Probing Two Holographic Models of Strongly Coupled Anisotropic Plasma,” arXiv:1205.4684 [hep-th].

- [35] P. Romatschke and M. Strickland, “Collisional energy loss of a heavy quark in an anisotropic quark-gluon plasma,” *Phys. Rev. D* **71** (2005) 125008 [hep-ph/0408275].
- [36] P. Romatschke, “Momentum broadening in an anisotropic plasma,” *Phys. Rev. C* **75** (2007) 014901 [hep-ph/0607327].
- [37] A. Dumitru, Y. Nara, B. Schenke and M. Strickland, “Jet broadening in unstable non-Abelian plasmas,” *Phys. Rev. C* **78** (2008) 024909 [arXiv:0710.1223 [hep-ph]].
- [38] M. E. Carrington, K. Deja and S. Mrowczynski, “Parton Energy Loss in an Unstable Quark-Gluon Plasma,” arXiv:1110.4846 [hep-ph].
- [39] A. Kurkela and G. D. Moore, “Thermalization in Weakly Coupled Nonabelian Plasmas,” *JHEP* **1112** (2011) 044 [arXiv:1107.5050 [hep-ph]].
- [40] P. M. Chesler, Y. -Y. Ho and K. Rajagopal, “Shining a Gluon Beam Through Quark-Gluon Plasma,” arXiv:1111.1691 [hep-th].